On the learning control effects in the cancer-immune system competition

Léon Masurel, Carlo Bianca, Annie Lemarchand

On the learning control effects in the cancer-immune system competition

Léon Masurel[1], Carlo Bianca[2], and Annie Lemarchand*[1]

[1] *Sorbonne Université, Centre National de la Recherche Scientifique (CNRS)*
Laboratoire de Physique Théorique de la Matière Condensée (LPTMC),
4 place Jussieu, case courrier 121, 75252 Paris Cedex 05, France

[2] *École Supérieure d'Ingénieurs en Génie Électrique, Productique et Management Industriel*
Laboratoire de Recherche en Eco-innovation Industrielle et Energétique,
13 Boulevard de l'Hautil, 95092 Cergy Pontoise Cedex, France

*Corresponding author: E-mail: anle@lptmc.jussieu.fr

Keywords: Kinetic theory, thermostat, direct simulation Monte Carlo, cell interactions

Abstract:

The interactions between a tumor and the immune system are modelled at cell scale in the framework of thermostatted kinetic theory. Cell activation and learning are reproduced by the increase of cell activity during interactions. The second moment of the activity of the whole system is controlled by a thermostat which reproduces the regulation of the learning process and memory loss through cell death. An algorithm inspired from the direct simulation Monte Carlo (DSMC) method is used to simulate stochastic trajectories for the numbers of cells and to study the sensitivity of the dynamics to various parameters. The nonintuitive role played by the thermostat is pointed out. For inefficient thermalization, the divergence of the number of cancer cells is obtained in spite of favored production of immune system cells. Conversely, when the activity fluctuations are controlled, the development of cancer is contained even for weakened immune defenses. These results may be correlated to unexpected clinical observations in the case of different cancers, such

as carcinoma, lymphoma, and melanoma.

1 Introduction

The treatment of cancer by boosting the immune system is a recent and promising therapeutic strategy [1, 2, 3]. Analogously to the immune system response to an infection, specific white blood cells are activated in the presence of antigens located on the surface of cancer cells [4, 5]. Recently, the role of dendritic cells as antigen presenting cells (APC) has been established. Usually an APC ingests and decomposes a non-self cell (e.g. pathogens, mushrooms) by isolating an antigen and presenting it to an immune system cell, a T lymphocyte [6]. The presentation process of the antigen to the T cell triggers the activation and then the proliferation of the T cells, thus allowing them to rid the human body of harmful cells. During the learning process developed by the T cells, the cancer cells can develop the ability to blend into the surrounding tissue and mislead the immune system cells [7, 8]. Thus the normal activation process of the T cells may not be sufficient to stop the onset and growth of the tumor. In particular, mutation processes can allow the cancer cells to avoid the surveillance of the immune system. An apparent elimination of the tumor may precede a long period of equilibrium, eventually followed by the proliferation of the cancer cells, according to a process identified as "the three E's" of immunoediting, for "Elimination, Equilibrium and Escape" [9].

Kinetic theory appears as a suitable framework to model cancer and immune system competition at the cell scale [10]. Originally designed to model dynamics of dilute gases [11, 12, 13, 14, 15], kinetic theory has been applied to granular materials [10] and biological systems [16]. The thermostatted kinetic theory has been proposed to model complex biological systems [17, 18, 19, 20, 21]. Accordingly, the activation and the learning of a cell are mimicked by increasing a quantity called activity and related to each cell. A thermostat term is introduced to account for the regulation of cell activity, in the spirit of the control of energy fluctuations in a dissipative system. Activity dissipation by the thermostat during the process of cell learning can be related to the action of regulatory T cells and natural cell death, which removes high activity cells from the system as well. Re-

cently the thermostatted kinetic theory has been employed to develop a minimal model involving three types of cells. The results showed that the model is able to reproduce the elimination of cancer cells, the equilibrium, and the escape from the immune system surveillance [22]. From the perspective of cancer immunotherapy optimization, the aim of the present paper is to perform a numerical sensitivity analysis, i.e. to study the impact of changes in each parameter on the cancer-immune system competition [2]. In particular the crucial role played by the thermostat term is pointed out.

The paper is organized as follows. Section 2 deals with the presentation of the model and the simulation method inspired from direct simulation Monte Carlo (DSMC) [13, 23]. Sections 3 to 7 are devoted to the results of a numerical sensitivity analysis. Specifically, the effect of the field of the thermostat is presented in Section 3, the total initial number of cells in Section 4, the rate constants associated with the interactions between a cancer cell and an immune system cell in Section 5, the initial numbers of cancer cells and immune system cells in Section 6, and the rate constant associated with the interactions between a cancer cell and a normal cell in Section 7. Finally, in section 8, we sum up the favorable conditions in which the model predicts tumor control by the immune system and draw conclusions in the context of cancer treatment.

2 The model

This section deals with the details of the model and the biological assumptions. Specifically, three types of cells are commonly involved in the immune response, the antigen-presenting cells, the T cells, and the B cells [4, 5]. A T cell is activated when it interacts with an antigen-presenting cell [6]. A subset of activated T cells transforms the B cells into plasma cells which secrete a large volume of antibodies. The antibodies then block antigen sites on the surface of cancer cells. Activated T cells may also mutate into T-killer cells, which destroy the cancer cells. When a cancer cell is killed, additional antigens are released, stimulating activation and learning of new T cells and B cells. While the T

cells are activated, cancer cells also mutate and develop the ability to avoid detection and destruction by the immune system. In particular, cancer cells may express proteins on their surface that induce immune cell inactivation and promote cancer cell proliferation. Finally, the regulatory T cells control the response of the immune system: They recognize anti-body coated cancer cells and adapt the level of antibody secretion, i.e. the regulation of the B-cell and the T-cell production and activation. In addition, cells have a limited lifespan leading to some memory loss of the global activation process.

In order to take into account the immune system response to cancer cells, we have recently proposed a minimal model of cell interactions and activation [19, 20, 21, 22]. Specifically, only three cell types are taken into consideration: Normal cells n, cancer cells c, and immune system cells i. Activation of both immune system cells and cancer cells is reasonably assumed to occur during binary interactions, like for example during the efficient contacts between a T cell and a dendritic cell with large surface-to-volume ratio. In the model, the level of activation is translated into the value reached by a quantity, u, accordingly named activity and carried by each cell. For an immune system cell, activity measures the degree of learning, gained by exposure to antigen. For a cancer cell, activity measures the degree of invisibility reached by mutation at the contact with immune system cells. The system is assumed to be spatially homogeneous and initial cell heterogeneity is reproduced by allocating to each cell an activity distributed according to a sufficiently large Gaussian distribution

$$P(u) = \frac{1}{\sigma\sqrt{2\pi}} \mathrm{e}^{-\left(\frac{u-\mu}{\sigma\sqrt{2}}\right)^2} \tag{1}$$

of mean value μ and standard deviation σ.

For the sake of simplicity, we consider that, regardless of cell types, all the interactions between two cells of different types systematically increase the activity by a same amount ϵ, for the cell with the largest activity u before interaction. The model introduces the following processes with rates that are assumed to depend on the difference of activities

between the interacting cells:

$$\begin{cases} c(u) + n(u') \overset{k_{cn}(u-u')H(u-u')}{\longrightarrow} c(u+\epsilon) + c(u') \\ \\ S \longrightarrow n(u'') \end{cases} \tag{2}$$

$$i(u) + c(u') \overset{k_{ic}(u-u')H(u-u')}{\longrightarrow} i(u+\epsilon) + i(u') \tag{3}$$

$$c(u) + i(u') \overset{k_{ci}(u-u')H(u-u')}{\longrightarrow} c(u+\epsilon) + c(u') \tag{4}$$

where k_{cn}, k_{ic} and k_{ci} are rate constants. The two indices of a rate constant refer to the two types of interacting cells, the first index corresponding to the type of the cell with the largest activity. The Heaviside step function $H(u-u')$, which is equal to 1 if $u > u'$ and otherwise vanishes, is introduced to ensure that only cell interactions with appropriate activities are considered. Hence, cancer cells proliferation may result from the interaction between a weakly activated cancer cell and a normal cell, as stated in Eq. (2). The system is supposed to be open and in contact with a source S of normal cells which maintains the number of normal cells constant. In order to mimic the strategy of cancer cells to avoid detection by the immune system, the autocatalytic production of cancer cells may also result from the interaction between a properly activated cancer cell and a less activated immune system cell, according to Eq. (4). Equation (3) expresses the attack of an activated killer T cell against a cancer cell and the subsequent T-cell proliferation and activation.

Regulation of immune system response and memory loss of activation through cell death are accounted for by a thermostat, so called by analogy with dissipation of energy in a system maintained at constant temperature [17, 18]. Usually, mathematical models for cancer-immune system competition derived within the kinetic theory framework are proposed under the assumption that the system is not at equilibrium [24]. In order to account for out-of-equilibrium conditions, the introduction of a thermostat term is fundamental.

The thermostat is associated with a field E, aiming at controlling the second moment $\langle u^2 \rangle$ of the activity of the total number of cells:

$$\frac{\mathrm{d}u}{\mathrm{dt}} = E - \alpha u \tag{5}$$

where the coefficient α reads:

$$\alpha = \frac{\langle u \rangle E}{\langle u^2 \rangle} \tag{6}$$

The kinetic equations governing the time evolution of the distribution functions associated with the three kinds of cells $j = n, i, c$ are given in the appendix [22].

In order to numerically solve the kinetic equations and additionally reproduce the internal fluctuations inherent to small systems, we have adapted the direct simulation Monte Carlo (DSMC) method, originally designed to solve the Boltzmann equation for dilute gases [13, 23]. The aim of the simulation is to follow the evolution of a small part of an organ in which some cancer cells already appeared. The initial state of the system is defined by the total number of cells N^0, the initial number, N_c^0, of cancer cells, and the initial number, N_i^0, of immune system cells. The number $N_n = N^0 - N_c^0 - N_i^0$ of normal cells remains constant but the total number N of cells may increase. Time is discretized. During the time step Δt, interactions between different types of cells and between the cells and the thermostat are successively performed.

An upper bound for the number of binary interactions between N cells during Δt is given by $r = N(N-1)k_{max}\Delta u_{max}\Delta t$, where k_{max} is the maximum rate constant among k_{cn}, k_{ic}, k_{ci} and where Δu_{max} is the maximum positive difference between the activities u and u' of two cells. First, r interactions between cells are tempted and accepted according to their probability of occurrence. For example, in the case of the process stated in Eq. (2), the interaction between a randomly chosen cell of cancer type $c(u)$ and a randomly chosen cell of normal type $n(u')$ is rejected if $u' > u$ and accepted proportionally to $\frac{k_{cn}(u-u')}{k_{max}\Delta u_{max}}$ if $u > u'$. Once the mutation of a normal cell $n(u')$ into a cancer cell $c(u')$ occurred, a normal cell $n(u'')$ is simultaneously introduced in the system with an activity u'' randomly chosen according to the probability $P(u)$ given in Eq. (1). Hence, the total

number N_n of normal cells remains constant. After an interaction has been accepted, the activities of the interacting cells and the numbers of cells of each type are updated as required by the considered process. The maximum difference of activities, Δu_{max}, is also updated.

Then, each cell interacts with the thermostat associated with the field E. Following Eqs. (5,6), we perform the update of the activity of each cell at each time step:

$$u(t+\Delta t) = u(t) + \Delta t E\Big(1 - \frac{\langle u\rangle}{\langle u^2\rangle}u(t)\Big) \tag{7}$$

where $\langle u\rangle$ and $\langle u^2\rangle$ are the mean value and the second moment of the activity of the whole system, which are updated at each time step.

The direct simulation Monte Carlo algorithm of thermostatted cell interactions is adapted to generate stochastic trajectories during a given total time t^{end} supposed to mimic life expectancy of a patient. In most simulations, the total simulation time is set to $t^{end}/\Delta t = 50000$ and the time step, to $\Delta t = 1$. For large values of the thermalizing field $E \simeq 1$, we impose $\Delta t = 10^{-2}$, in order to satisfy the condition $E\Delta t \ll 1$.

The Gaussian probability distribution $P(u)$ of the initial cell activity stated in Eq. (1) is characterized by the mean value $\mu = 0.5$ and the standard deviation $\sigma = 0.2$. The increase of activity during the cell-cell interaction is equal to $\epsilon = 10^{-3}$, small compared to the standard deviation σ. As shown in Fig. 1, three different types of stochastic trajectories are obtained for given parameter values, simply by changing the seed of the random number generator. Figure 1a illustrates the case where the final number, $N_c^{end} = 0$, of the cancer cells vanishes and the final number, N_i^{end}, of immune system cells reaches a stationary non-vanishing value. This case can be interpreted as cancer elimination by the immune system. Figure 1b gives an example of coexistence, where $N_c(t)$ and $N_i(t)$ fluctuate around nonvanishing values until t^{end}: The immune system is said to control the cancer during life expectancy. The paradoxical coexistence of cancer cells and T cells remains a subject of debate [25]. In Fig. 1c, the final number, $N_i^{end} = 0$, of immune system cells vanishes and the number of cancer cells diverges. This last case is typical of

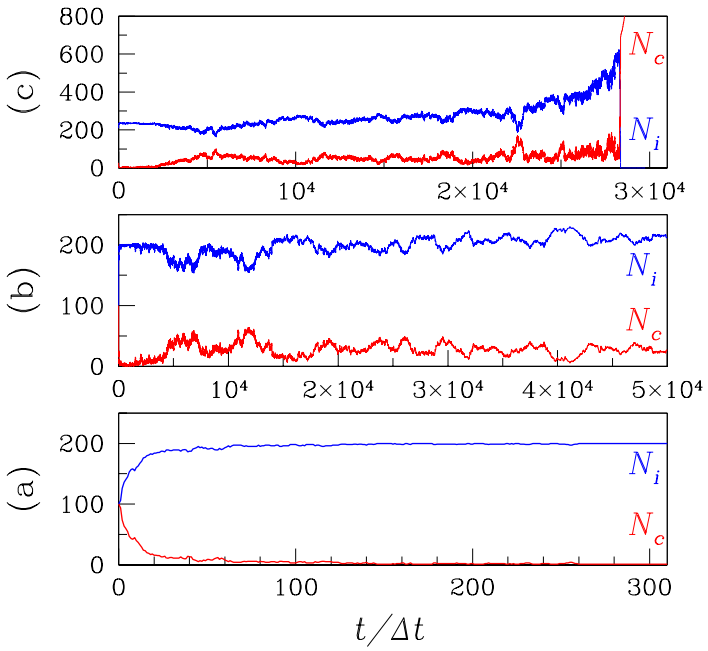

Figure 1: The three typical kinds of evolutions of the numbers, N_c, of cancer cells (red) and numbers, N_i, of immune system cells (blue) obtained for three different seeds of the random number generator and $N^0 = 10^3$, $N_c^0 = 100$, $N_i^0 = 100$, $E = 2.5 \times 10^{-4}$, $k_{ic} = 10^{-2} > k_{ci} = 10^{-3}$, $k_{cn} = 10^{-6}$. (a) Fast elimination of the cancer cells: $N_c^{end} = 0$. (b) Coexistence: The immune system controls the tumor for the duration of the simulation: $N_c^{end} N_i^{end} \neq 0$. (c) Escape of cancer from immunosurveillance: $N_i^{end} = 0$ and the number of cancer cells diverges.

cancer escape from immune system control.

In the next sections, we provide a comprehensive overview of the effect of all the relevant parameters on the evolution of the number, N_c, of cancer cells and, N_i, of immune system cells, in order to propose a possible optimization strategy of cancer immunosurveillance. The rate constant k_{cn}, which controls the interaction between cancer cells and normal cells, is fixed at a lower value than k_{ic} and k_{ci} except otherwise stated. Indeed, small values of k_{cn} prevent the proliferation of the total number of cells and better reveal the sensitivity of the system to the other parmeters. The effect of k_{cn} variation is studied in section 7.

3 Effect of the field E of the thermostat

The field E controls the activity dissipation related to the memory loss in the process of cell learning. The effect of the thermostat mimics natural cell death, which removes high activity cells from the system as well. The role of moderator played by the thermostat in the model also reproduces the action of regulatory T cells, able to modulate the immune system by downregulating proliferation and activation of T cells. The probabilities of occurrence of the three different behaviors shown in Fig. 1 are given in Fig. 2 for variable different values of E.

In the limit of no dissipation, i.e. as E tends to 0, only the two extreme cases associated with either $N_c^{end} = 0$ or $N_i^{end} = 0$ are observed. For $E < 10^{-4}$, 20% of the simulated cases lead to cancer elimination, whereas cancer proliferates in 80% of the cases. The conditions for modifying the respective percentages of cancer elimination and proliferation will be discussed in section 6. As illustrated in Fig. 1a, the cases leading to $N_c^{end} = 0$ are observed as a fluctuation accidentally induces the vanishing of N_c. The number of immune system cells then remains equal to the value reached at the time for which N_c vanishes. This event may arise at short times, since the number of cancer cells rapidly reaches small values in the chosen conditions, in particular, for $k_{ic} > k_{ci}$. The influence of the rate constant values on the behavior of the system will be studied in section 5. As illustrated in Fig. 1c, the cases corresponding to $N_i^{end} = 0$ surprisingly occur after the increase of the number of immune system cells. However, the increase of N_i is associated with the increase of anticorrelated fluctuations for N_i and N_c: A large fluctuation inducing a large decrease and vanishing of N_i may occur before the end of the simulation. Once N_i vanishes, cancer cells proliferate and N_c diverges. Figure 1c gives an example of the three E's of immunoediting [9]: On a very short time scale, cancer seems to be eliminated, then remains at quasiequilibrium, but finally escapes from immunosurveillance.

In the limit of large dissipation, for $E > 4 \times 10^{-4}$, all the simulated trajectories lead to the same type of final state with nonvanishing numbers of cancer cells and immune system cells, as shown in Fig. 2. For sufficiently large values of the field E, efficient thermalization

decreases the fluctuation level of the activity u: The risk of observing a large fluctuation inducing either $N_c = 0$ or $N_i = 0$ during the simulation time is smaller. The system is stabilized in an apparently stationary state with slightly fluctuating nonvanishing values of N_c and N_i. The nondiverging final values of the numbers of cancer cells and immune system cells and the maximum values reached during the simulation time are displayed in Fig. 2 for variable E values in the two most probable cases. The cases leading to $N_c^{end} = 0$ are omitted. In the limit of no dissipation, for $E < 10^{-4}$, the maximum number N_i^{max} of immune system cells is large compared to the final value $N_i^{end} = 0$, whereas, for large field values $E > 4 \times 10^{-4}$, the final number N_i^{end} and the maximum number N_i^{max} of immune system cells nearly coincide. It is also clear in Fig. 2 that, for $E > 4 \times 10^{-4}$ and $k_{ic} > k_{ci}$, the final number N_i^{end} of immune system cells is larger than the final number N_c^{end} of cancer cells. This point will be addressed again in section 5.

According to Fig. 2, an abrupt bifurcation occurs for a critical value $E^{cr} \sim 2.5 \times 10^{-4}$ of the field: For small field values, $E < E^{cr}$, 80% of the cases end with $N_i^{end} = 0$ and cancer proliferates. For large field values, $E > E^{cr}$, all the cases lead to a control of the tumor. As expected, the fluctuations are amplified in the vicinity of the bifurcation and N_i^{max} increases close to E^{cr} [26]. Figure 3 gives the distributions of the waiting time t_i for reaching $N_i^{end} = 0$ in the domain $E < E^{cr}$. The distributions become larger as $E \to E^{cr}$ and the increase of the mean waiting time $\langle t_i \rangle$ is made explicit in Fig. 3.

As a result, we conclude that the effect of thermalization, i.e. the control of activity fluctuations, is favorable to cancer surveillance. For values of the field E larger than a critical value, the cancer cells are not eliminated but their number remains bounded during the simulation time, interpreted as the life expectancy of the patient. The cancer is controlled in a sufficiently dissipative system where the fluctuations of activity are regulated. Dissipation of activity occurs through cell death. Although regulatory T cells are known to suppress T cell and hinder the immune response against cancer, their thermalizing role could explain why high levels of regulatory T cells may be associated with a positive prognosis, for example in the case of colorectal carcinoma and follicular

lymphoma [27, 28].

4 Effect of the total initial number N^0 of cells

The initial number of normal cells, N_n^0, mimics the size of the organ affected by the tumor. Assuming that the initial numbers of immune system cells, N_i^0, and cancer cells, N_c^0, are small compared to N_n^0, we vary the total number of cells $N^0 = N_n^0 + N_i^0 + N_c^0$ at constant N_i^0 and N_c^0 in order to evaluate the impact of the organ size on cancer evolution. The specific effects of N_i^0 and N_c^0 will be discussed in section 6. The sensitivity of the system to N^0 is enhanced in the vicinity of the bifurcation, close to the critical value $E^{cr} \sim 2.5 \times 10^{-4}$ of the thermalizing field. Figure 4 shows the influence of N^0 on the behavior of the system for $E \sim E^{cr}$. The probability for observing a total elimination of the cancer does not change and remains equal to 20% regardless of the value of N^0. A bifurcation occurs for a critical value $N^{0,cr} \sim 10^3$ of the initial number of cells: 80% of the cases lead to cancer proliferation ($N_i^{end} = 0$) for large initial numbers of cells, $N^0 > N^{0,cr}$, and to cancer control ($N_i^{end} N_i^{end} \neq 0$) for small initial numbers of cells, $N^0 < N^{0,cr}$. This result may seem counterintuitive, since the fluctuations usually regress in the so-called thermodynamic limit, associated with large values of the total number of particles. For small values of the rate constant k_{cn} associated with the contamination of normal cells by cancer cells, the final total number N of cells remains close to the initial number N^0. The behavior observed in Fig. 4 for $N^0 \ll N^{0,cr}$ and $E \sim E^{cr}$ is close to the one obtained in Fig. 2 for $N^0 \sim N^{0,cr}$ and $E \gg E^{cr}$. Analogously, the behavior observed for $N^0 \gg N^{0,cr}$ and $E \sim E^{cr}$ is close to the one obtained for $N^0 \sim N^{0,cr}$ and $E \ll E^{cr}$. Hence, decreasing the total initial number N^0 of cells has a similar effect as increasing the thermalizing field E. The same conclusion holds when comparing the variation of the mean waiting time $\langle t_i \rangle$ for reaching $N_i^{end} = 0$ in Fig. 3 and Fig. 5. A better thermalization and smaller fluctuations are obtained in a small system, as confirmed by the smaller maximum values N_i^{max} reached as N^0 decreases in Fig. 5. A better control of the tumor is then achieved when the number of cells that can be potentially damaged is smaller.

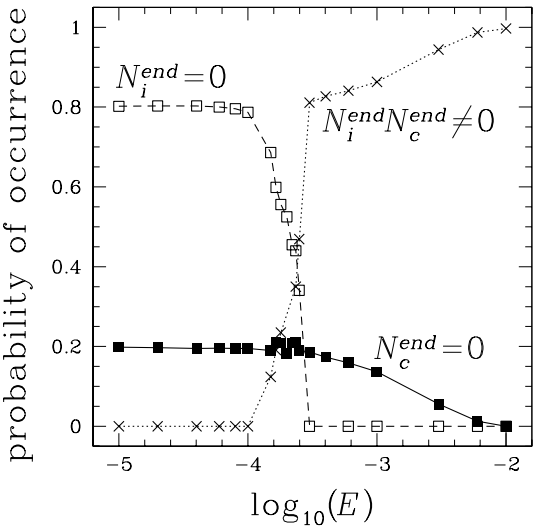

(a)

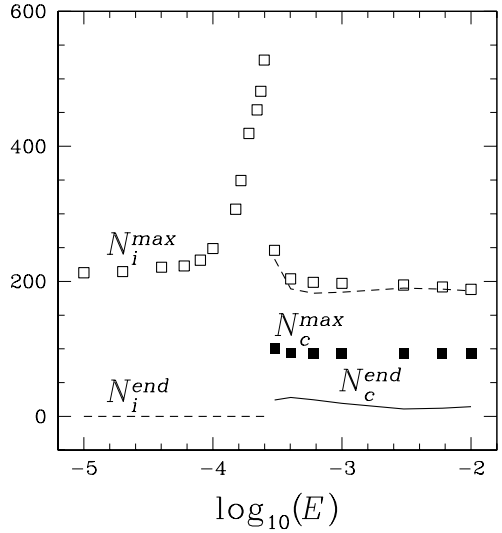

(b)

Figure 2: (a) Probability of occurrence of the three cases shown in Fig. 1 for $k_{ic} = 10^{-2} > k_{ci} = 10^{-3}$ versus common logarithm $\log_{10}(E)$ of the field E associated with the thermostat. Solid line and solid squares: Elimination of the cancer cells ($N_c^{end} = 0$). Dotted line and crosses: Control of the cancer ($N_c^{end}N_i^{end} \neq 0$). Dashed line and open squares: Escape of cancer from immunosurveillance ($N_i^{end} = 0$). (b) Final and maximum values of different numbers of cells versus common logarithm $\log_{10}(E)$ in the two most probable cases leading either to $N_c^{end}N_i^{end} \neq 0$ or to $N_i^{end} = 0$. Dashed line: Final values of the number N_i^{end} of immune system cells. Solid line: Final values of the number N_c^{end} of cancer cells. Open squares: Maximum values of the number N_i^{max} of immune system cells. Solid squares: Maximum values of the number N_c^{max} of cancer cells. The other parameter values are given in the caption of Fig. 1.

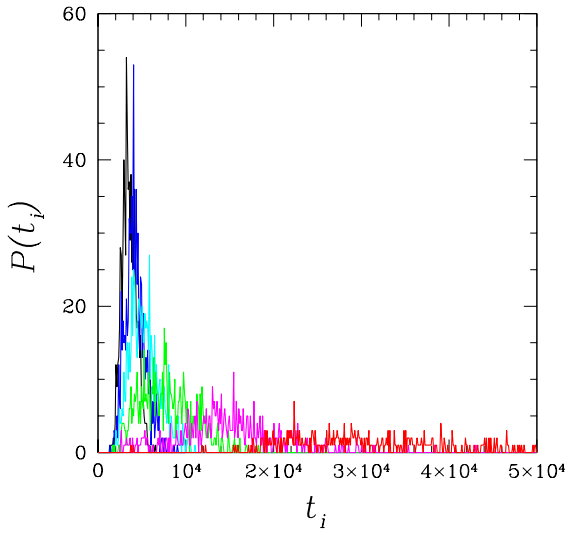

(a)

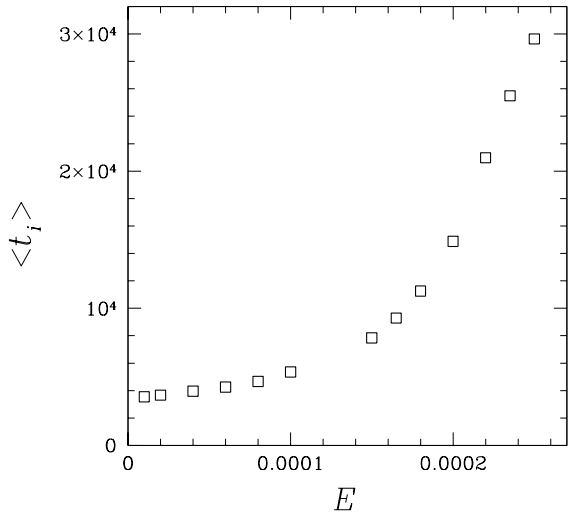

(b)

Figure 3: (a) Distributions of waiting times t_i for reaching $N_i^{end} = 0$ for different values of the field E associated with the thermostat, $E = 10^{-5}$ (black), $E = 6 \times 10^{-5}$ (blue), $E = 10^{-4}$ (cyan), $E = 1.5 \times 10^{-4}$ (green), $E = 2 \times 10^{-4}$ (magenta), and $E = 2.5 \times 10^{-4}$ (red). (b) Mean waiting time $\langle t_i \rangle$ for reaching $N_i^{end} = 0$ versus field E associated with the thermostat. The other parameter values are given in the caption of Fig. 1, in particular, $N^0 = 10^3$.

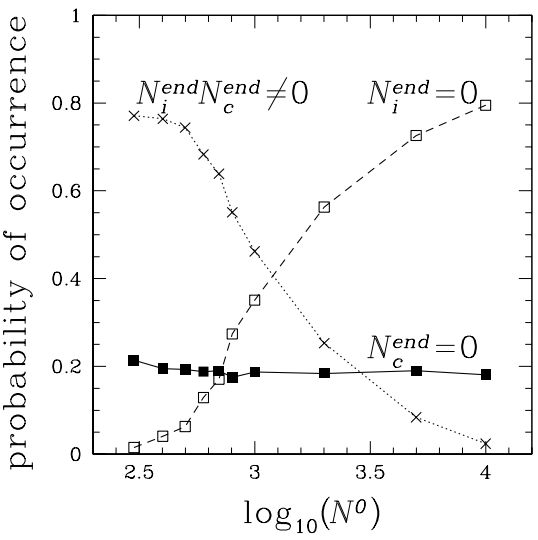

Figure 4: Probability of occurrence of the three cases shown in Fig. 1 versus common logarithm $\log_{10}(N^0)$ of the total initial number of cells. Solid line and solid squares: Elimination of the cancer cells ($N_c^{end} = 0$). Dotted line and crosses: Control of the tumor ($N_c^{end} N_i^{end} \neq 0$). Dashed line and open squares: Escape of cancer from immunosurveillance ($N_i^{end} = 0$). The other parameter values are given in the caption of Fig. 1, in particular, $E = 2.5 \times 10^{-4}$.

Hence, the results of the model for different initial numbers N^0 of cells and close to the critical value of the thermalizing field satisfactorily reproduce that a tumor, specific to an organ and without risk of dissemination, is more likely to be defeated. It is worth noting that the sensitivity of the system to N^0 disappears for noncritical field values.

5 Effect of the rate constants k_{ic} and k_{ci}

The rate constant k_{ic} is associated with the autocatalytic production of immune system cells according to Eq. (3) and the rate constant k_{ci} is associated with the autocatalytic production of cancer cells according to Eq. (4). The comparison between Fig. 2, obtained for $k_{ic} = 10^{-2}$ and $k_{ci} = 10^{-3}$, and Fig. 6, obtained for $k_{ic} = 10^{-3}$ and $k_{ci} = 10^{-2}$, reveals that a bifurcation occurs for the same critical value $E = E^{cr}$ of the field. The probabilities for observing a final state with nonvanishing numbers of immune system cells and cancer cells vary in the same way, regardless of the exchange of the values of k_{ic} and k_{ci}. For sufficiently large values $E \gg E^{cr}$ of the field, cancer control is observed in 100% of the

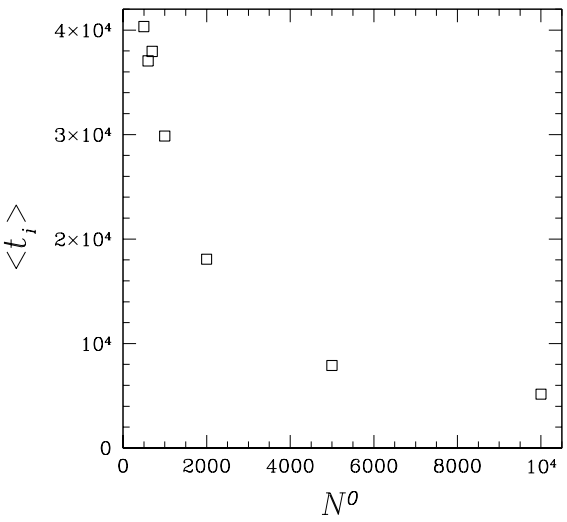

(a)

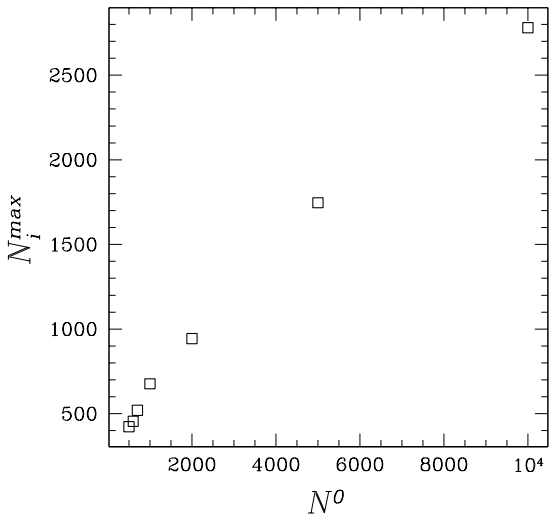

(b)

Figure 5: (a) Mean waiting time $\langle t_i \rangle$ for reaching $N_i^{end} = 0$ versus total initial number N^0 of cells. (b) Maximum value $N_i^{\max}$ of the number of immune system cells reached during the evolution versus total initial number N^0 of cells. The other parameter values are given in the caption of Fig. 1, in particular, $E = 2.5 \times 10^{-4}$.

cases. For $E \gg E^{cr}$, the order relation between the final numbers of cells, N_c^{end} and N_i^{end}, is intuitive: As shown in Fig. 6, a value of the rate constant k_{ci} associated with the autocatalytic production of cancer cells larger than k_{ic} leads to final values N_c^{end} of cancer cells larger than the final values N_i^{end} of immune system cells. Without surprise, the case $k_{ic} > k_{ci}$ studied in Fig. 2 is leading to the opposite result.

For small values, $E \ll E^{cr}$, of the field, the exchange between the values of k_{ic} and k_{ci} leads to the exchange between the probabilities of occurrence of $N_c^{end} = 0$ and $N_i^{end} = 0$. In particular, 20% of the cases lead to cancer elimination ($N_c^{end} = 0$) if $k_{ic} > k_{ci}$ and to destruction of all immune system cells ($N_i^{end} = 0$) if $k_{ic} < k_{ci}$. Similarly, for $E \ll E^{cr}$, 80% of the cases lead to $N_i^{end} = 0$ if $k_{ic} > k_{ci}$ and to $N_c^{end} = 0$ if $k_{ic} < k_{ci}$. A larger value of the rate constant k_{ci} associated with the production of cancer cells according to Eq. (4) is more favorable to cancer eradication. This counterintuitive result is obtained for an inefficient thermostat, for which larger cell numbers are correlated with larger fluctuations, i.e. larger N_c^{max} values as shown in Fig. 6. Consequently, the probability that an accidental fluctuation leads to $N_c^{end} = 0$ is larger for $k_{ic} < k_{ci}$. Similarly, the probability that a fluctuation leads to $N_i^{end} = 0$ is larger for $k_{ic} > k_{ci}$.

Hence, a larger production rate of immune system cells is favorable to cancer control in a well-regulated system. The final numbers of cancer cells remain smaller than the number of immune system cells for $k_{ic} > k_{ci}$ and $E > E^{cr}$: Cancer is well controlled during life expectancy when immune system cells rapidly form. If the effect of the regulatory T cells is small or, more generally, if dissipation is too weak, stimulating the production of immune system cells may be counterproductive. Opposite results from those sought may be achieved, due to large fluctuations of cell number and activities, leading to probable vanishing of the number of immune system cells and cancer proliferation.

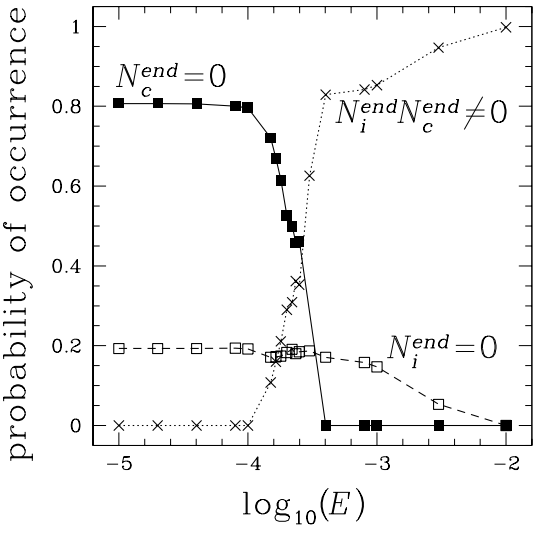

(a)

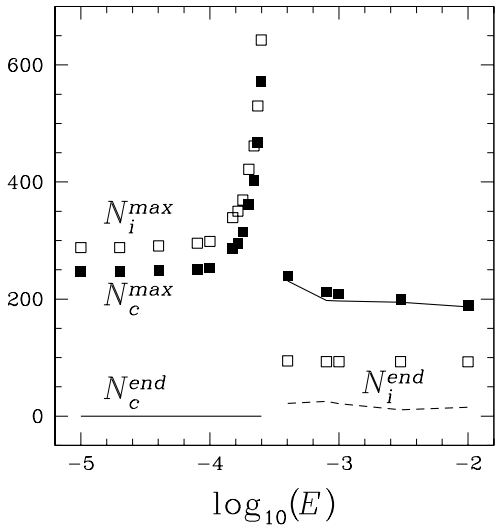

(b)

Figure 6: (a) Probability of occurrence of three typical evolutions versus common logarithm $\log_{10}(E)$ of the field E associated with the thermostat. Solid line and solid squares: Elimination of the cancer cells ($N_c^{end} = 0$). Dotted line and crosses: Control of the tumor ($N_c^{end} N_i^{end} \neq 0$). Dashed line and open squares: Escape of cancer from immunosurveillance ($N_i^{end} = 0$). (b) Final and maximum values of different number of cells versus common logarithm $\log_{10}(E)$ in the two most probable cases observed in the top subfigure. Dashed line: Final values of the number N_i^{end} of immune system cells. Solid line: Final values of the number N_c^{end} of cancer cells. Open squares: Maximum values of the number N_i^{max} of immune system cells. Solid squares: Maximum values of the number N_c^{max} of cancer cells. Same parameter values as in Fig. 2 except $k_{ic} = 10^{-3} < k_{ci} = 10^{-2}$.

6 Effect of the initial numbers N_c^0 of cancer cells and N_i^0 of immune system cells

The initial number N_c^0 of cancer cells mimics the size of the tumor at the instant where immunotherapy starts with N_i^0 immune system cells. Close to the critical value, $N^{0,cr} \sim 10^3$, of the initial number of cells and for a small field value, $E \ll E^{cr}$, the probabilities of occurrence of the three cases, cancer elimination ($N_c^{end} = 0$), cancer control ($N_c^{end} N_i^{end} \neq 0$), and cancer proliferation ($N_i^{end} = 0$), vary with the initial numbers N_c^0 of cancer cells and N_i^0 of immune system cells, as shown in Fig. 7. More precisely, for the chosen parameter values, the probability for observing $N_c^{end} N_i^{end} \neq 0$ remains equal to 0, regardless of the values of N_c^0 and N_i^0. The probability for obtaining $N_i^{end} = 0$ monotonically decreases as N_i^0 increases and N_c^0 decreases. The probability for obtaining $N_c^{end} = 0$ monotonically increases as N_i^0 increases and N_c^0 decreases. In the whole range of variation, $0 < N_c^0 < N^0 - N_i^0$ and $0 < N_i^0 < N^0 - N_c^0$, of the initial cell numbers, very close values of the probabilities of occurrence of the difference cases are found for constant $(N_i^0)^2/N_c^0$ values. It means that, under inefficient regulation conditions, a first patient with initially N_c^0 cancer cells and N_i^0 immune system cells and a second patient, which has initially four times the number of cancer cells, have the same chance to eradicate cancer provided the initial number of immune system cells of the second patient is twice as large as N_i^0.

As shown in Fig. 7 for the same parameter values but in a well-thermostatted system with a large field $E \gg E^{cr}$, the probabilities of occurrence of the three different cases remain unchanged as N_c^0 and N_i^0 vary. In the entire domain of explored $(N_i^0)^2/N_c^0$ values, nearly 100% of the cases lead to cancer control with $N_c^{end} N_i^{end} \neq 0$. Figure 8 makes explicit how the final values N_c^{end} and N_i^{end} vary as N_c^0 and N_i^0 are changed. We find that the value of N_i^{end} remains small and unchanged whereas N_c^{end} varies like $N_i^0 + N_c^0$. Contrary to intuition, a larger initial value N_i^0 of immune system cells leads to a larger final value N_c^{end} of cancer cells. This result is actually obtained in the case where the rate constant k_{ic} associated with the production of immune system cells is smaller than the

rate constant k_{ci} associated with the production of cancer cells, as already shown in Fig. 6 and discussed in section 5. For the same parameter values but $k_{ic} > k_{ci}$, N_c^{end} remains small and constant as N_c^{end} and N_i^{end} vary and N_i^{end} is close to $N_i^0 + N_c^0$.

7 Effect of the rate constant k_{cn}

The rate constant k_{cn} controls the rate of the autocatalytic production of cancer cells from the interaction between a cancer cell and a normal cell. When the mutation occurs, the reservoir S is solicited to inject a new normal cell into the system, which increases the total number of cells. The results given in the previous sections are obtained for the value $k_{cn} = 10^{-6}$, smaller than the considered values of the rate constants k_{ic} and k_{ci}. We now examine the properties of the system for a larger value $k_{cn} = 10^{-3}$, of the order of magnitude of k_{ic} and k_{ci}. According to Fig. 6 obtained for $k_{cn} = 10^{-6}$ and omitting the less probable case ending with $N_i^{end} = 0$, we find that dynamics is ending with $N_c^{end} = 0$ for $E < E^{cr}$ and with $N_c^{end} N_i^{end} \neq 0$ for $E > E^{cr}$. Such a bifurcation does not exist for $k_{cn} = 10^{-3}$ and all the simulated trajectories end with $N_c^{end} N_i^{end} \neq 0$, regardless of the field value. As shown in Fig. 9, a transition is nevertheless observed for $E^{tr} \simeq 10^{-2}$, with large values of N_c^{end} andN_i^{end} for $E < E^{tr}$ and small values of N_c^{end} andN_i^{end} for $E > E^{tr}$.

Hence, large k_{cn} values lead to a considerable increase of the total number of cells N for small field values, $E < E^{tr}$. A priori, large values of k_{cn} may be suspected of inducing proliferation of cancer cells. However, large k_{cn} values favor the fast introduction of new normal cells with an activity close to the mean value and the fast destruction of low activity normal cells. The decrease of the relative activity between cancer cells and immune system cells counterbalances the increase of k_{cn}, so that the production rate of cancer cells remains bounded. Larger values of both N_c and N_i lead to smaller fluctuations of these quantities and smaller risk that the evolution ends with vanishing or diverging N_c values.

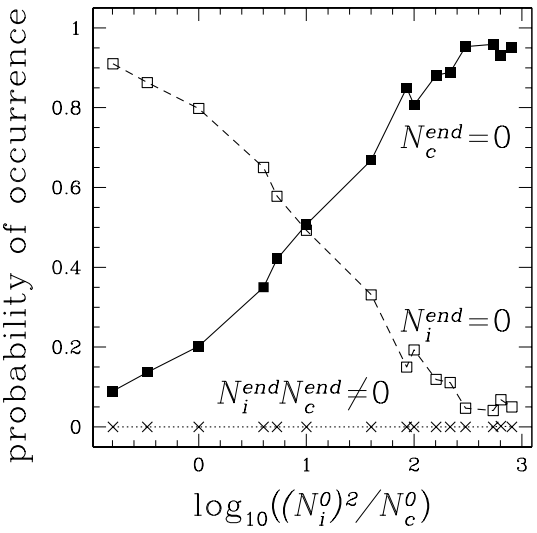

(a)

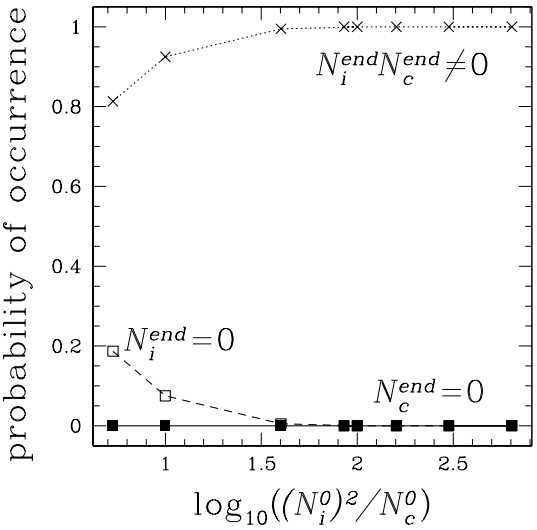

(b)

Figure 7: (a) Probability of occurrence of three typical evolutions versus common logarithm $\log_{10}((N_i^0)^2/N_c^0)$ for $N^0 = 10^3$, $E = 10^{-5}$, $k_{ic} = 10^{-3} < k_{ci} = 10^{-2}$. Solid line and solid squares: Elimination of the cancer cells ($N_c^{end} = 0$). Dotted line and crosses: Control of the tumor ($N_c^{end}N_i^{end} \neq 0$). Dashed line and open squares: Escape of cancer from immunosurveillance ($N_i^{end} = 0$). (b) Same caption for except $E = 10^{-2}$.

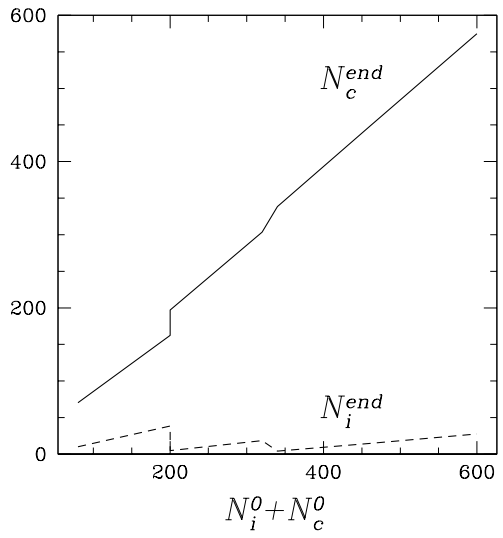

Figure 8: Variation of the final numbers of cancer cells, N_c^{end}, and immune system cells, N_i^{end}, versus the sum $N_c^0 + N_i^0$ of the initial numbers of cancer cells, N_c^0, and immune system cells, N_i^0 in the case where $N_c^{end} N_i^{end} \neq 0$. The parameter take the following values $N^0 = 10^3$, $E = 10^{-2}$, $k_{ic} = 10^{-3} < k_{ci} = 10^{-2}$.

On the contrary, the final number of cells remains close to the initial one N^0 for $E > E^{tr}$. Then, the behavior is similar to the one observed in Fig. 6 for $E > E^{cr}$ and $k_{cn} = 10^{-6}$: 100% of the simulated trajectories end with $N_c^{end} N_i^{end} \neq 0$, $N_i^{end} \ll N_c^{end}$ and $N_c^{end} \simeq N_c^0 + N_i^0$ for $k_{ic} < k_{ci}$, regardless of the value of the rate constant k_{cn}. In addition, above E^{tr}, the symmetry between the exchange of k_{ic} and k_{ci}, on the one hand, and the exchange of N_i^{end} and N_c^{end}, on the other hand is observed, for small as for large k_{cn} values. Simply, as k_{cn} decreases, the transition occurs for a larger value E^{tr} of the field.

To sum up this section, we note that the behavior of the system is not sensitive to the value of the rate constant k_{cn}, provided that the field is sufficiently large. For an inefficient thermostat $E < E^{tr}$ and for $k_{ic} < k_{ci}$, small k_{cn} values may predominantly lead to unexpected recovery as shown in Fig. 6, but large k_{cn} values result in the more intuitive development of the tumor with final values N_c^{end} of cancer cells much larger than the initial total number of cells, N^0, as shown in Fig. 9. It is worth noting that, however, N_c^{end} does not diverge. Large k_{cn} values act as a thermostat with respect to the control

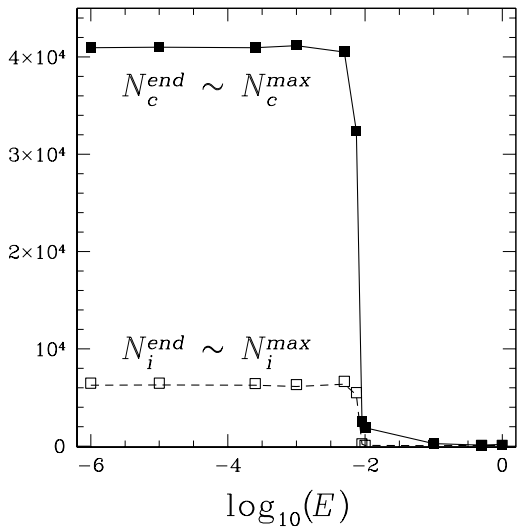

Figure 9: Final and maximum values of different numbers of cells versus common logarithm $\log_{10}(E)$ for the same parameter values ($N^0 = 10^3$, $N_c^0 = 100$, $N_i^0 = 100$, $k_{ic} = 10^{-3}$, $k_{ci} = 10^{-2}$) as in Fig. 6 except $k_{cn} = 10^{-3}$. The time step is set to $\Delta t = 0.01$ for $E \in [0.011]$. Dashed line: Final values of the number N_i^{end} of immune system cells. Solid line: Final values of the number N_c^{end} of cancer cells. Open squares: Maximum values of the number N_i^{max} of immune system cells. Solid squares: Maximum values of the number N_c^{max} of cancer cells.

of the number of cells. Analogous conclusions hold for $k_{ic} > k_{ci}$, provided N_c^{end} and N_i^{end} are exchanged. Large field values $E > E^{tr}$ are favorable to the control of the tumor and warrant small final numbers N_c^{end} of cancer cells that are independent of k_{cn}.

8 Conclusion

In this paper, the interactions between a tumor and the immune system are described at the cell scale in the framework of thermostatted kinetic theory. We choose a model of cell interactions having already given qualitative account of the three 3E's of immunoediting [9]: Elimination, equilibrium, and escape from immune system control are reproduced [22]. Cell interactions may modify cell type and cell activity, a quantity accounting for the level of learning of immune system cells exposed to antigens as well as the degree of invisibility reached by cancer cells. Interestingly, memory loss related to cell death and regulation of the immune system are reproduced by the effect of a "thermostat", which regulates

activity fluctuations in an analogous way as an actual thermostat controls temperature fluctuations. An algorithm inspired by the direct simulation Monte Carlo method [13, 23] is used to numerically solve the kinetic equations for the probability densities of normal cells, cancer cells, and immune system cells. The simulations generate stochastic trajectories for the numbers of cells and the activity of the system. We study the effect of the various parameters of the model on the dynamics of the system. The total initial number of cells, the initial numbers of cancer cells and immune system cells, the rate constants, and the field of the thermostat are varied. The effect on the final numbers of cancer cells and immune system cells are discussed.

According to the results, the key parameters accounting for different behaviors observed in immunotherapy are the rate constant k_{cn} associated with the interactions between a cancer cell and a normal cell and the field E of the thermostat. These two parameters have similar, nonintuitive effects, related to their control of fluctuations. If either k_{cn} or E is large, the final number of cancer cells N_c^{end} never diverges. For large k_{cn} values, the total number of cells sensitively increase, due to the increase of the number of either cancer cells if k_{ci} is large or immune system cells if k_{ic} is large. Then, the usual decrease of fluctuation level is observed in the presence of a large number of interacting objects. A large field E, i.e. an efficient thermostat, leads to a good control of activity variance, suppresses large fluctuations of cell activities and numbers. The probability to accidentally observe a vanishing final number of immune system cells $N_i^{end} = 0$ decreases and the final number of cancer cells N_c^{end} unlikely diverges. The positive impact of the thermostat on cancer control compares well with clinical observations. Indeed, patients with high levels of regulatory T-cell expression have a better chance of healing in the case of colorectal carcinoma and follicular lymphoma [27, 28]. Although regulatory T cells decrease the number of immune system cells, their positive impact on the disease can be interpreted as a control over cell number and consequently, a thermalizing role. For larger values of E, the final state is less sensitive to the other parameters and even independent

of the initial number of cells N^0. Expected results are then obtained: A more favorable outcome, i.e. a smaller final number of cancer cells N_c^{end}, is obtained for (i) a larger rate constant k_{ic} associated with the production of immune system cells than the rate constant k_{ci} associated with the production of cancer cells, (ii) a smaller initial number of cancer cells N_c^0, (iii) a larger initial number of immune system cells N_i^0 provided N_i^0 increases as $\sqrt{N_c^0}$.

On the contrary, for small values of both the field E and the rate constant k_{cn}, large fluctuations develop. Contrary to usual findings, a smaller initial total number of involved cells N^0 then leads to smaller fluctuations of the different cell numbers and a smaller risk to accidentally end with $N_i^{end} = 0$. The case $k_{ic} > k_{ci}$, although associated with the faster production of immune system cells, is unfavorable because larger values of the number N_i of immune system cells correlate with larger fluctuations of this quantity and, consequently, an increased probability to observe a vanishing final number of immune system cells $N_i^{end} = 0$. Thermalization mimics dissipation of information and small thermalization reproduces cells with long lifespan or efficient learning, for immune system cells but also cancer cells. This last result may explain the poor performance of immunotherapy in the case of some patients, for which mutations of cancer cells, all the more likely as cell life is long, may induce adaptive resistance to the treatment [29].

In conclusion, our model of cell interactions based on thermostatted kinetic theory accounts for observed clinical behaviors, including unexpected healing induced by weakened immune defenses as well as proliferation of the tumor in spite of favored production of immune system cells.

Appendix: Kinetic equations governing the evolution of the distribution functions associated with the three kinds of cells

Distribution functions $f_j(t, u)$ depending on time and activity for each kind of cells $j = n, i, c$ are introduced in the framework of kinetic theory. According to the thermostatted

kinetic approach introduced in references [19, 20, 21], the time evolution of the distribution functions $f_j(t,u)$ obey:

$$\partial_t f_j(t,u) + \partial_u \left(F(u) f_j\right) = I_j \tag{8}$$

where $F(u)$ is associated with the thermostat and I_j is the interaction term affecting the cells of type j and resulting from the processes given in Eqs. (2-4). Specifically, the interaction term I_c related to the cancer cells is given by:

$$\begin{aligned} I_c &= \int_{\mathbb{R}^+} k_{cn}(u-\epsilon-u')H(u-\epsilon-u')f_c(t,u-\epsilon)f_n(t,u')\mathrm{d}u' \\ &+ \int_{\mathbb{R}^+} k_{cn}(u'-u)H(u'-u)f_c(t,u')f_n(t,u)\mathrm{d}u' \\ &- \int_{\mathbb{R}^+} k_{ic}(u'-u)H(u'-u)f_c(t,u)f_i(t,u')\mathrm{d}u' \\ &+ \int_{\mathbb{R}^+} k_{ci}(u-\epsilon-u')H(u-\epsilon-u')f_c(t,u-\epsilon)f_i(t,u')\mathrm{d}u' \\ &+ \int_{\mathbb{R}^+} k_{ci}(u'-u)H(u'-u)f_c(t,u')f_i(t,u)\mathrm{d}u' \end{aligned} \tag{9}$$

The first and second integrals refer to the autocatalytic generation of cancer cells by Eq. (2), the third integral refers to the destruction of cancer cells according to Eq. (3), and the fourth and fifth integrals refer to the autocatalytic production of cancer cells by Eq. (4). Similarly, the interaction term I_i associated with the immune system cells is:

$$\begin{aligned} I_i &= \int_{\mathbb{R}^+} k_{ic}(u-\epsilon-u')H(u-\epsilon-u')f_c(t,u')f_i(t,u-\epsilon)\mathrm{d}u' \\ &+ \int_{\mathbb{R}^+} k_{ic}(u'-u)H(u'-u)f_c(t,u)f_i(t,u')\mathrm{d}u' \\ &- \int_{\mathbb{R}^+} k_{ci}(u'-u)H(u'-u)f_c(t,u')f_i(t,u)\mathrm{d}u' \end{aligned} \tag{10}$$

The first and second integrals refer to the autocatalytic production of immune system cells due to the process given in Eq. (3) and the third integral is related to tumor counterattack of immune system cells according to Eq. (4). Finally, the interaction term I_n for the normal cells reads:

$$\begin{aligned} I_n &= -\int_{\mathbb{R}^+} k_{cn}(u'-u)H(u'-u)f_c(t,u')f_n(t,u)\mathrm{d}u' \\ &+ P(u)\int_{\mathbb{R}^+}\int_{\mathbb{R}^+} k_{cn}(u'-u)H(u'-u'')f_c(t,u')f_n(t,u'')\mathrm{d}u'\mathrm{d}u'' \end{aligned} \tag{11}$$

The first integral originates from the mutation of normal cells by the process given in Eq. (2) and the second integral accounts for the effect of the source of normal cells with activities distributed according to the normalized distribution $P(u)$ given in Eq. (1). By integrating Eq. (8) over u for $j = n$, we obtain $\partial_t \int_{\mathbb{R}^+} f_n(t,u)\mathrm{d}u = 0$ and check that the density $\rho_n = \int_{\mathbb{R}^+} f_n(t,u)du$ of normal cells is actually kept constant.

Due to the mutation of normal cells into cancer cells and the simultaneous re-injection of normal cells into the system through the process given in Eq. (2), the total number of cells increases. Hence, the sum of the interaction terms does not vanish:

$$\sum_{j=n,i,c} I_j \neq 0 \tag{12}$$

and the second moment of the activity,

$$\langle u^2 \rangle = \int_{\mathbb{R}^+} u^2 \sum_{j=n,i,c} f_j(t,u)\mathrm{d}u \tag{13}$$

is not strictly conserved. However, in order to prevent an explosion of activity fluctuations and for the sake of simplicity, we introduce the same thermostat, as if the total number of cells was conserved. By analogy with the coefficient of friction α introduced in Eqs. (5,6), we look for a thermostat term in the form $F(u) = E - \alpha u$ in Eq. (8) and obtain:

$$F(u) = E\left[1 - u\int_{\mathbb{R}^+} u\left(\sum_{j=n,i,c} f_j(t,u)\right)\mathrm{d}u\right] \tag{14}$$

The integration of the distribution function $f_j(t,u)$ associated with cell type j over the activity u gives the density of j cells. Macroscopic equations for the densities of cells have been derived by performing either a low-field or a high-field scaling and considering the related convergence when the scaling parameter goes to zero. Specifically, we have proven that the macroscopic equations show diffusion with respect to both space and activity in the low-field limit [20, 21]. The direct simulation of the kinetic equations provides stochastic trajectories for the number of cells. The simulations not only give access to the deterministic evolution of the densities of cells but also include the description of their fluctuations.

Declarations of interest: none.

References

[1] T. Blankenstein, P. G. Coulie, E. Gilboa and E. M. Jaffee, Nat. Rev. Cancer **12**, 307 (2012).

[2] M. D. Vesely and R. D. Schreiber, Ann. N.Y. Acad. Sci. **1284**, 1 (2013).

[3] I. Sagiv-Barfi, D. K. Czerwinski, S. Levy, I. S. Alam, A. T. Mayer, S. S. Gambhir, and R. Levy, Sci. Transl. Med. **Vol. 10, Issue 426** (2018) DOI: 10.1126/scitranslmed.aan4488.

[4] C. A. Siegrist, in *Vaccines* (5th ed), edited by S. A. Plotkin, W. A. Orenstein, and P. A. Offit (Saunders Elsevier, New York, 2008) pp. 17-36.

[5] O. Leo, A. Cunningham, P. L. Stern in *Understanding Modern Vaccine, Perspectives in Vaccinology*, Vol. 1, edited by N. Garçon and P. L. Stern (Elsevier B. V., Amsterdam, 2011) pp. 25-59.

[6] P. Guermonprez, J. Valladeau, L. Zitvogel, C. Thry, and S. Amigorena, Annu. Rev. Immunol. **20**, 621 (2002).

[7] G. P. Dunn, A. T. Bruce, H. Ikeda, L. J. Old and R. D. Schreiber, Nature immunology **3**, 991 (2002).

[8] F. H. Igney and P. H. Krammer, J. Leukoc. Biol. **71**, 907 (2002).

[9] G. P. Dunn, L. J. Old and R. D. Schreiber, Annu. Rev. Immunol. **22**, 329 (2004).

[10] C. Cercignani, *Recent results in the kinetic theory of granular materials*, in Perspectives and problems in nonlinear science, ed. E. Kaplan, J. E. Marsden, and K. R. Sreenivasan, pp. 217228 (Springer, New York, 2003).

[11] M. Kac, in *The Boltzmann equation, theory and applications*, edited by E. G. D. Cohen and W. Thirring, Volume 10 of the series Acta Physica Austriaca (Springer, Vienna, 1973) pp. 379-400.

[12] C. Cercignani, R. Illner and M. Pulvirenti, *The mathematical theory of dilute gases* (Springer, New York, 1994).

[13] G. A. Bird, *Molecular Gas Dynamics and the Direct Simulation of Gas Flows* (Clarendon, Oxford, 1994).

[14] A. Lemarchand and B. Nowakowski, Phys. Rev. E **62**, 3156 (2000).

[15] B. Nowakowski and A. Lemarchand Phys. Rev. E **68**, 031105 (2003).

[16] P. Dziekan, A. Lemarchand and B. Nowakowski J. Chem. Phys. **137**, 074107 (2012).

[17] B. Wennberg and Y. Wondmagegne, J. Stat. Phys. **124**, 859 (2006).

[18] C. Bianca, Nonlinear Analysis: Real World Applications **13**, 2593 (2012).

[19] C. Bianca and C. Dogbe, Nonlinearity **27**, 2771 (2014).

[20] C. Bianca and A. Lemarchand, Communications in Nonlinear Science and Numerical Simulation **20**, 14 (2015).

[21] C. Bianca, C. Dogbe and A. Lemarchand, Acta Applicandae Mathematicae **189**, 1 (2015).

[22] C. Bianca and A. Lemarchand, J. Chem. Phys. **145**, 154108, (2016).

[23] F. Alexander and A. Garcia, Computers in Physics **11**, 588 (1997).

[24] N. Bellomo, C. Bianca, and M. Delitala, Physics of Life Reviews **6**, 144 (2009).

[25] G. Marincola and F. M. Marincola, in Immunotherapy of Cancer, ed. Mary L. Disis, p. 317 (Humana Press, Totowa, 2006).

[26] G. Nicolis and I. Prigogine, *Self-Organization in Nonequilibrium Systems* (Wiley, New York, 1977).

[27] J. Wang and X.-Y. Ke, J. Hematol. Oncol. **4**, 50 (2011).

[28] K.-S. Le, M.-L. Thibult, S. Just-Landi, S. Pastor, F. Gondois-Rey, S. Granjeaud, F. Broussais, R. Bouabdallah, R. Colisson, C. Caux, C. Mntrier-Caux, D. Leroux, L. Xerri, and D. Olive, Cancer Res. **76**, 4648 (2016).

[29] J. M. Zaretsky, A. Garcia-Diaz, D. S. Shin, H. Escuin-Ordinas, W. Hugo, S. Hu-Lieskovan, D. Y. Torrejon, G. Abril-Rodriguez, S. Sandoval, L. Barthly, J. Saco, B. Homet Moreno, R. Mezzadra, B. Chmielowski, K. Ruchalski, I. P. Shintaku, P. J. Sanchez, C. Puig-Saus, G. Cherry, E. Seja, X. Kong, J. Pang, B. Berent-Maoz, B. Comin-Anduix T. G. Graeber, P. C. Tumeh, T. N. Schumacher, R. S. Lo, A. Ribas, N. Engl. J. Med. **375**, 819 (2016).